CHAPTER V
IMPACTS OF CHANNEL STRUCTURE AND OXIDE PROMOTERS ON PETROCHEMICAL AND FUEL PRODUCTIONS FROM BIO-ETHANOL DEHYDRATION USING HZSM-11 AND HZSM-5 DOPED WITH GROUP 5A - OXIDES

5.1 Abstracts

HZSM-5 has been widely used in ethanol dehydration which its pore size govern the product distributions. In our previous work, it was shown that the gasoline- and kerosene- range products were mainly obtained by using HZSM-5 that has the zigzag channel structure. Moreover, P-, Sb-, and Bi- oxides supported on HZSM-5 have been found to improve oil yields, C9-, and C10+ aromatic productions. With an equivalent pore size, HZSM-11 which has the straight channel structure, and HZSM-5 were thus used in order to investigate the effect of channel structure on the bio-ethanol dehydration. Moreover, P-, Sb-, and Bi- oxides were doped as a promoter, aiming to study the effects on production of valuable hydrocarbons as well. The bio-ethanol dehydration was conducted at 500 °C, and the LHSV was fixed at 0.5 h^{-1} HZSM-5 (SiO_2/Al_2O_3 ratio = 80) and HZSM-11 (SiO_2/Al_2O_3 ratio = 75) with/without 5 % P-, Sb- and Bi- oxide loading (elemental basis) were used as catalysts. The catalysts were characterized using XRD, SAA, and XPS. The oil products were examined using GC, GCxGC-MS/TOF, and SIMDIST GC. As a result, more C9 and C10+ aromatics were produced by using HZSM-5(80). On the other hand, HZSM-11 produced BTEX with high propylene selectivity. P_xO_y/zeolite improved oxygenates and C10+ aromatics, while Sb_xO_y/zeolite increased benzene and toluene selectivity. Bi_xO_y/HZSM-11 can improve the BTEX production, while Bi_xO_y/HZSM-5 produced mainly non-aromatics. Pore channel structure affected dominantly to oil yields, and HZSM-5(80) produced 7.69% higher oil yields than HZSM-11(75).

5.2 Introduction

Bio-ethanol can be the one of natural source of chemical feedstock that can fulfill the world chemical consumption. Nowadays, bio-ethanol was widely used in fuel application. Moreover, bio-ethanol dehydration was reported to convert to hydrocarbons including gas and oil. Bio-ethanol can be converted to ethylene (Lu *et al.*, 2011) and propylene (Goto *et al.*, 2010). Moreover, the oil products, which contains BTEX and other hydrocarbons, produced by using HZSM-5 as a catalyst were derived in many cases. Viswanadham *et al.* (2012) investigated the effects of particle size and SiO_2/Al_2O_3 ratio of HZSM-5, and revealed that the C8 aromatic selectivity and oil yields obtained by using HZSM-5(30) were higher than using HZSM-5(100). On the other hand, HZSM-5(100) yielded greater property of oil, considered by the RON number, than HZSM-5(30). In addition, HZSM-11 is a zeolite that has the pore size close to that of HZSM-5, but they are different in pore channel structure. HZSM-11 has the straight channel structure, however; HZSM-5 has both straight and zigzag channel structure. In order to compare effect of channel structures, Gu *et al.* (2012) studied the HZSM-5, H-Beta, HY, nano HZSM-5, HZSM-11, and nano HZSM-11 on glycerol dehydration to acrolein. They found that the nano HZSM-11 showed the best performance in glycerol dehydration to acrolein, which gave 81.6% conversion and 79.4% selectivity to acrolein at 8 hr time-on-stream. HZSM-11 also gave a great yield of aromatics in 1-hexene aromatization and isomerization at 370 °C. In addition, HZSM-11 showed better performance than HZSM-5 even with less strong acid strength than HZSM-5 because ZSM-11 has the only straight pore channel; therefore, the product can easily moved out of the pore. At the same particle size and SiO_2/Al_2O_3 ratio, the selectivity of aromatics was 70.8% and 78.9% by using HZSM-5 and HZSM-11, respectively (Zhang *et al.*, 2010). Varvarin *et al.* (2013) also studied the effect of pore size and pore structure on n-butanol dehydration to hydrocarbons by using HZSM-5, HZSM-11, H-L, and H-Y zeolites at 250-400 °C under atmospheric pressure. The differences between the yield of liquid hydrocarbons of HZSM-5 and HZSM-11 were not significant. HZSM-5 and HZSM-11 can produce the aromatic yield of 67 mol% and 62 mol%, respectively at 400°C. Moreover, the main products for HL and HY zeolites were alkenes. HL and HY zeolites can give 39 mol% and 34 mol% alkenes yield, respectively.

Pure HZSM-5 had the limit in oil production, so a promoter can improve the oil yield. In our previous work, the improvement of the aromatics was revealed by Pasomsub (2013). He studied the ZSM-5 loaded by group 5A oxides in the highest oxidation state (X_2O_5 where X is P, Sb, or Bi) at 1%, 2%, 3%, and 4% loading can improve the xylene, ethylbenzene ,C9 and C10+ aromatic yields. However, when P_2O_5 was added to ZSM-5, the selectivity of p-xylene, ethylbenzene, C9 and C10+ aromatics increased while that of benzene, toluene, and m-xylene decreased. The p-xylene reached the maximum at 3%P_2O_5 loading on HZSM-5. The yield of oil decreased with the increased loading of P_2O_5, opposite to the yield of gas. The gaseous products mainly consisted of ethylene and C3 hydrocarbons. The ethylene selectivity tended to increase; however, C3 hydrocarbons tended to decrease with the increased loading amount of P_2O_5 on HZSM-5. In addition, 2%Sb_2O_5 on HZSM-5 can produce the maximum oil yield. Sb_2O_5 on HZSM-5 can suppress toluene, benzene, and m-xylene formation. The selectivity of ethylbenzene can reach the maximum at 1% loading of Sb_2O_5 on HZSM-5. The kerosene range product increased with the increasing amount of Sb_2O_5 loading. The gaseous C3 hydrocarbons also decreased with the increasing loading of Sb_2O_5. On the other hand, ethylene selectivity increased with the increasing loading of Sb_2O_5. Bi_2O_5 on HZSM-5 gave the same trend as P_2O_5 and Sb_2O_5 in terms of suppressing the benzene and toluene selectivity and improving the C9 and C10+ aromatics. Xylenes selectivity decreased with the increasing Bi_2O_5 contents, which was different from that of P_2O_5 and Sb_2O_5 on HZSM-5. From the aforementioned, P_2O_5, Sb_2O_5, and Bi_2O_5 can improve the acid property of HZSM-5, leading to the increases in the C9 and C10+ formation and the suppression of m-xylene, toluene and benzene selectivity at the same time. However, P_2O_5/HZSM-5 showed more selectivity of C9 aromatics than C10+ aromatics because their mild acid strength that cannot further protonate to C10+ aromatics. The gaseous product mainly consisted of ethylene and C3 hydrocarbons. C3 hydrocarbons usually crack to a lighter molecule (such as ethylene) or react to a larger molecule (such as aromatic products). In addition, Wongwanichsin (2013) studied the antimony oxide at 3% and 5% loading on SAPO-34. He found that 5% antimony oxide (Sb_2O_3) on SAPO-34 can give 77.5% selectivity of C10+ aromatics while the unloaded SAPO-34 did not produce the

C10+ aromatic product. For the analysis of petroleum fractions, 5% Sb_2O_3 on SAPO-34 also produced 97.1% selectivity of gasoline range product while the unloaded SAPO-34 did not produce any liquid product. So, in this work, the effects of pore channel structure and promoters on the catalytic dehydration of bio-ethanol were investigated by using HZSM-5 and HZSM-11 as catalysts promoted with phosphorus oxide, antimony oxide, and bismuth oxide.

5.3 Experiment

5.3.1 Catalyst preparation

HZSM-5 zeolite (MFI, NH_4-form, SiO_2/Al_2O_3 = 80 mol/mol, BET surface area = 425 m^2/g, was purchased from Zeolyst International, USA), and HZSM-11 was synthesized by the same method as proposed by Chu *et al.* (1973) with some modifications. Sodium aluminate (technical anhydrous grade, Sigma Aldrich), Ludox HS-30 colloidal silica (sigma aldrich), and Tetrabutylammonium bromide (TBABr) (Reagent plus, Sigma Aldrich) were used as an alumina source, silica source, and template, respectively. HZSM-5 and HZSM-11 were calcined at 500 °C with the scanning rate of 5 °C/min for 3 hours to get the H-form zeolite and remove the impurity. The diammonium hydrogen phosphate ($(NH_4)_2HPO_4$, CARLO ERBA), antimony trichloride ($SbCl_3$, CARLO ERBA), and bismuth trichloride ($BiCl_3$, ALDRICH) were used as the source of P, Sb, and Bi, respectively. A solution of these compounds was individually loaded on the HZSM-5 and HZSM-11 supports using the incipient wetness impregnation technique to obtain 5 %wt loading elemental basis. Then, all catalysts were dried in the oven at 100 °C for 3 hours, followed by calcination in a flow of air at the same condition as applied to pure zeolites. The prepared catalysts were pelletized, ground, and sieved (20-40 mesh) for use in catalytic bio-ethanol dehydration process. The nomenclature of catalysts used in the experiment is shown in Table 5.1.

5.3.2 Catalyst Characterization

The surface area (BET), pore volume (HK), and pore size (HK) were determined based on N_2 physisorption using the Thermo Finnigan/Sorptomatic 1990. Crystallographic spectra of the zeolites were determined using Rigaku SmartLab® in

BB/Dtex mode with CuKα radiation. The machine collected from the 2θ of 5^{o} – 90^{o}, with the rate of 10^{o}/min, and the increment at 0.01.

Table 5.1 Nomenclature of catalysts used in the experiments

# of run	Catalyst	Abbreviation
1	HZSM-5(SiO_2/Al_2O_3 = 80)	HZ5(80)
2	HZSM-11(SiO_2/Al_2O_3 = 78)	HZ11(75)
3	5% Phosphorus oxide / HZSM-5(SiO_2/Al_2O_3 = 80)	P/HZ5(80)
4	5% Antimony oxide / HZSM-5(SiO_2/Al_2O_3 = 80)	Sb/HZ5(80)
5	5% Bismuth oxide / HZSM-5(SiO_2/Al_2O_3 = 80)	Bi/HZ5(80)
6	5% Phosphorus oxide / HBeta(SiO_2/Al_2O_3 = 78)	P/HZ11(75)
7	5% Antimony oxide / HBeta(SiO_2/Al_2O_3 = 78)	Sb/HZ11(75)
8	5% Bismuth oxide / HBeta(SiO_2/Al_2O_3 = 78)	Bi/HZ11(75)

XPS was used to determine the oxidation states of metal oxides dispersed in zeolites. The scan pass energy was 160 kv for wide scan and 40 kv for narrow scan. The electron source was Al Kα that gave 10 mA of emission and 15 kV of anode HT. The neutralizer was set at 1.8 A of filament current, 2.6 V of charge balance, and 1.3 V of filament bias. The amount of elemental loading on zeolite was determined by using XRF (AXIOS PW4400) with the radiation at 50 kv 60 mA.

5.3.3 Bio-ethanol dehydration

The fuel grade bio-ethanol (99.5% purity) was obtained from Sapthip co., ltd., Thailand. The catalytic dehydration of bio-ethanol was conducted in a U-tube fixed bed reactor (10 mm, inside diameter and 45.8 cm, length) under atmospheric pressure at 500^{o}C for 8 hours. Helium was used as a carrier gas fed at 13.725 ml/min. Bio-ethanol was fed at 2 ml/hour. 3 grams of catalyst was used in the reaction. The gas product was analyzed by using a GC-TCD (Agilent 6890N) to determine the gas compositions, and a GC-FID (Agilent 6890N) was used to determine the ethanol concentration in gas stream. The liquid product was condensed in the collector, immerged in an ice-salt bath, and then the oil phase was extracted from the liquid product using CS_2. The oil was analyzed by using GC×GC-TOFMS (Rxi-5SilMS, and RXi-17) to determine its composition. Moreover, the true boiling point curve of oil was determined by using SIMDIST GC. The range of boiling

points indicates the type of petroleum products; <120 °C for gasoline, 149-232 °C for kerosene, 232-343 °C for gas oil, 343-371 °C for light vacuum gas oil, and >371 °C for high vacuum gas oil (Pasomsup, 2013).

5.4 Results and Discussion

5.4.1 Catalyst Characterization

Table 5.2 Surface area, pore volume, and pore diameter

Catalyst	Surface area (m^2/g) [a]	Pore volume (cm^3/g) [b]	Pore diameter (Å) [b]	SiO_2/Al_2O_3 ratio [c]
HZ5(80)	357.35	0.1803	5.950	74.2
P/HZ5(80)	165.68	0.082	7.552	74.5
Sb/HZ5(80)	348.02	0.1708	5.918	74.6
Bi/HZ5(80)	332.31	0.1705	6.265	73.1
HZ11(75)	225.74	0.1103	5.950	74.8
P/HZ11(75)	112.98	0.0564	7.620	74.4
Sb/HZ11(75)	159.22	0.0864	6.522	73.7
Bi/HZ11(75)	154.21	0.0771	6.909	74.2

[a] determined using BET method

[b] determined using HK method, [c] determined by XRF

The BET surface area and pore volume decrease when all zeolites are doped with group 5A oxides as shown in Table 5.2. A large metal molecular weight in oxide leads to a large decrease in surface area and pore volume, except phosphorus doping. The small molecular size of phosphorus oxide leads to the high deposition in the pore of zeolite, so, the surface area and pore volume highly decrease. This behavior applies to all zeolite supports.

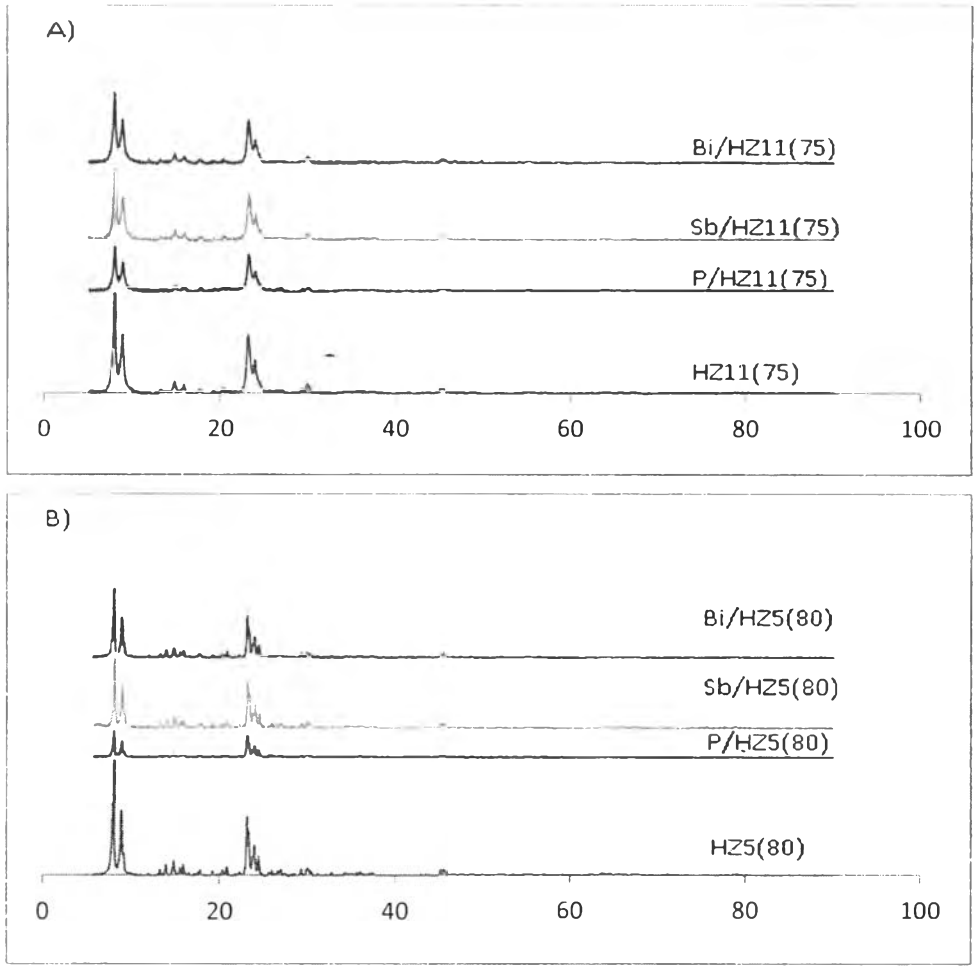

Figure 5.1 XRD spectra of phosphorus oxide-, antimony oxide-, and bismuth oxide-modified (A) HZSM-11, and (B) HZSM-5.

The XRD spectra are shown in Figure 5.1. The characteristic peaks of HZSM-11 are 7.954°, 8.838°, 14.841°, 23.211°, and 24.000° (Beck and Schlenker, 1993) and those of HZSM-5 are 7.94°, 8.87°, 14.70° - 14.88° (doublet), 20.34°, 23.68°, and 23.91° (Feng-Yuen *et al.*, 1988). The XRD patterns of pure zeolites and corresponding modified zeolites show the same 2θ of identity peaks. So, the structures of the zeolites were not destroyed by the modification.

The oxidation state of oxides on the modified zeolites is determined by using XPS, and the results are shown in Figure 5.2. The XPS spectra of phosphorus oxide-modified catalysts illustrate the P $2p_{3/2}$ positions at 135.8, 134.7,

133.3, 132.4 eV that can be interpreted to P_4O_{10}, metaphosphate, pyrophosphate, and phosphate, respectively (Moulder *et al.*, 1992).

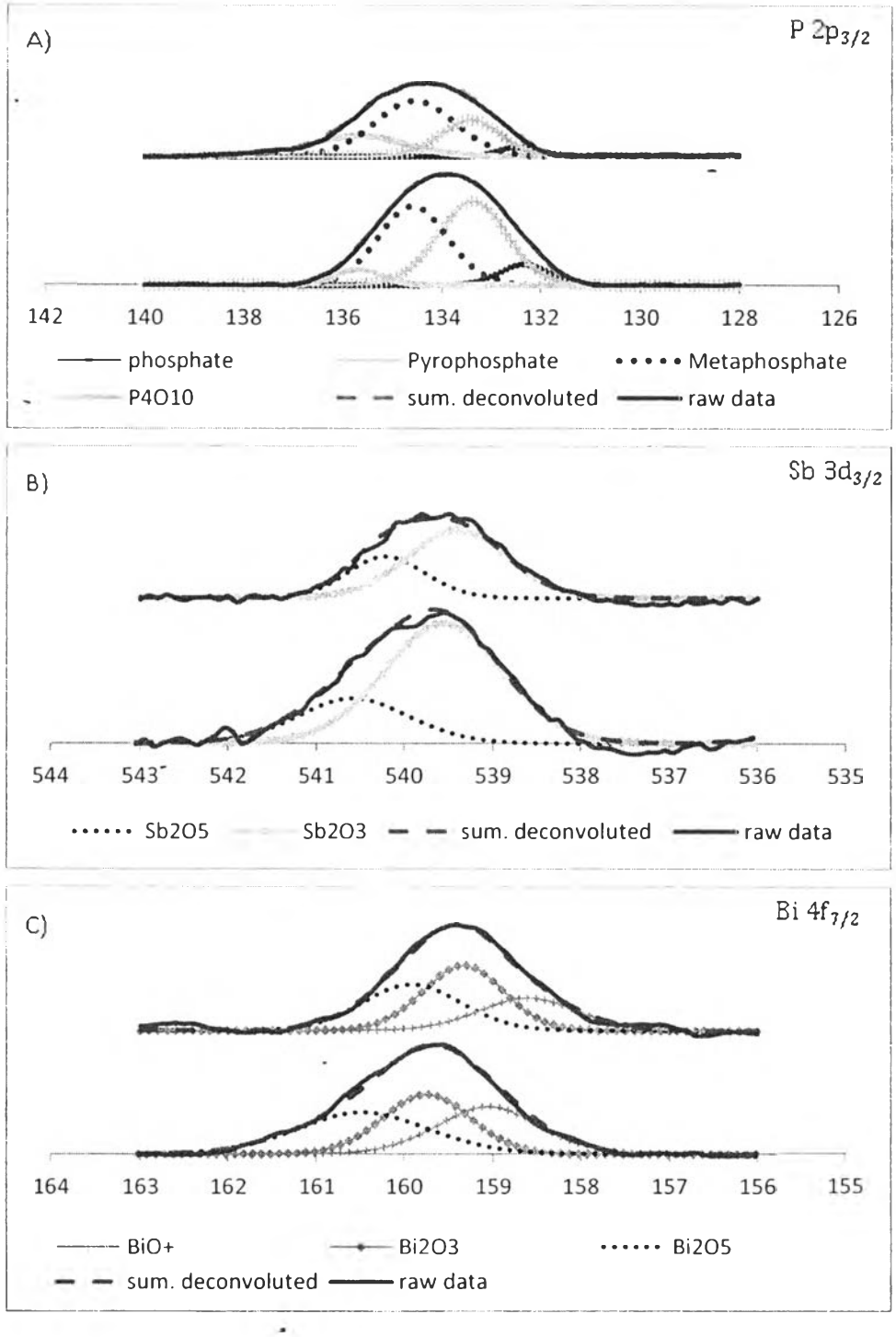

Figure 5.2 XPS spectra of (A) phosphorus oxide-, (B) antimony oxide-, and (C) bismuth oxide-doped catalysts.

Antimony oxide forms are shown in Figure 5.2 B. The Sb $3d_{5/2}$ spectrum was found to overlap with O 1s that occurs at 531.0 eV (Moulder *et al.*, 1992). Therefore, the spectrum of Sb $3d_{3/2}$ was employed to identify the oxide phases of antimony oxide. Zhang *et al.* (2013) reported that the Sb $3d_{3/2}$ peaks at 540.4 eV and 539.6 eV can be interpreted to Sb_2O_5 and Sb_2O_3, respectively. From Figure 5.2B, the Sb $3d_{3/2}$ spectra of antimony oxide-supported zeolites appear at 539.5 and 540.3 eV, which can be interpreted to Sb_2O_3 and Sb_2O_5, respectively. The results show that antimony oxide on HZ5(80) is composed of 67.6% Sb_2O_3 and 32.4% Sb_2O_5 whereas the one on HZ11(75) contains the mixture of 65.7% Sb_2O_3 and 34.2% Sb_2O_5. The phase compositions of oxide in both cases are not significantly different, and both Sb_2O_3 and Sb_2O_5 are mutually contributed to catalytic activity. Bismuth oxide-modified catalysts mainly contain Bi_2O_3 whose peak is located at 159.2 while other spectra appear at 160.4, 158.8 eV that refer to Bi_2O_5 and BiO_3^+, respectively (Li *et al.*, 2012).

5.4.2 Effect of Zeolite Pore Structure

In this case, HZSM-11 and HZSM-5 with the comparable pore size and SiO_2/Al_2O_3 ratio were used in order to investigate the effect of pore structure, which mean the zigzag pore structure of HZSM-5 and the straight pore of HZSM-11 was compared. Figure 5.3 show the pore channel structures of HZSM-11 and HZSM-5 at the miller indexes of [100] and [010].

Ethanol dehydration is conducted, and 95.5% and 97.7% conversion were achieved by using HZ5(80) and HZ11(75) catalysts, respectively, as shown in Figure 5.4. HZ11(75) gave the yields of 4.20% oil, 26.9% non-oil, and 68.9% gas, however; HZ5(80) gave the high yields of oil, which is 11.9%. The ratios of oil: non-oil: gas are 1:6.37:16.3 and 1:1.89:5.51 by using HZ11(75) and HZ5(80), respectively.

Light olefins consisting of 66.9% ethylene and 22.2% propylene are produced by using HZ11(75), while other gas products are produced in small extents as shown in Figure 5.5. The ratio of ethylene: propylene: other gases is 1:0.33:0.16. On the other hand, HZ(80) gave 43.17% propane selectivity.

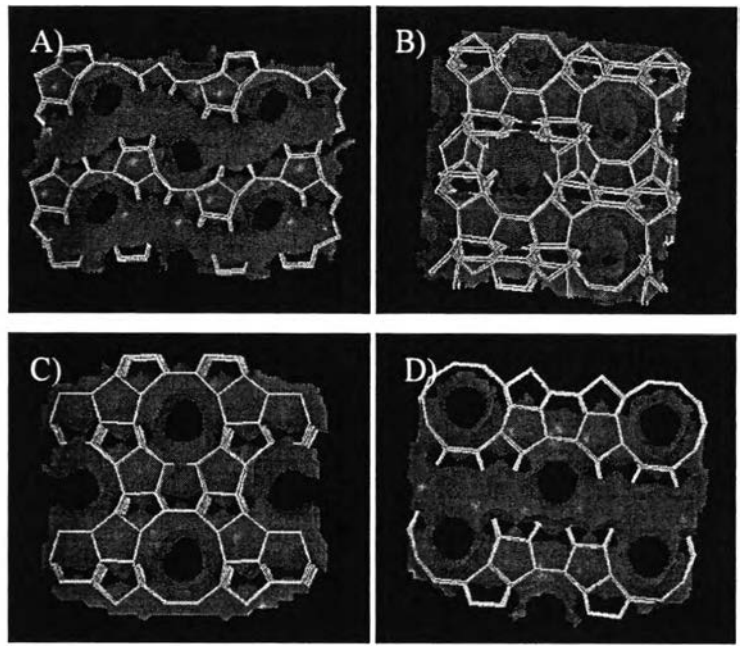

Figure 5.3 Pore channel structure of (A)HZSM-5 [010], (B)HZSM-5 [100], (C)HZSM-5 [010], and (D)HZSM-11 [100] (Baerlocher and McCusker, 2007).

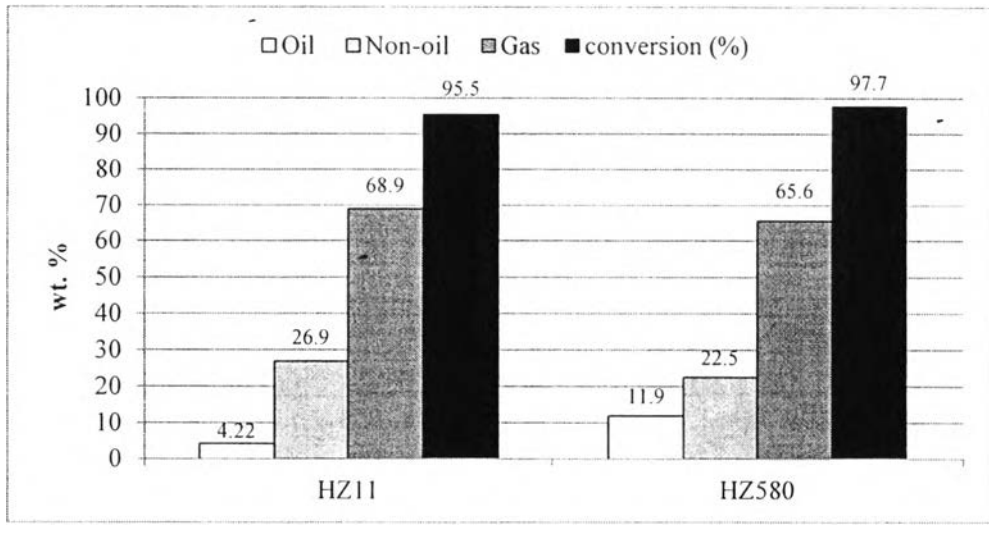

Figure 5.4 Product distribution and ethanol conversion from using HZ11(75), and HZ5(80) zeolite.

The high propane selectivity in gas can be attributed to the high catalytic activity in aromatization and dehydrocyclization because hydrogen from

those reactions can be localized to light olefin molecules to form light paraffins. C2 and C3 selectivity also indicate the catalytic activity. In case of using HZ5(80), C3 selectivity is higher than C2, which can be ascribed to the high catalytic activity in oligomerization and β-scission.

Acid density was controlled by using nearly the same SiO_2/Al_2O_3 of HZ11(75) and HZ5(80). One of the factors that affect the product distribution and oil yields was a complexity of zeolite channel structure. The results from the straight channel (0.53×0.54 nm) of HZ11(75) is compared with those from the straight channel (0.51×0.55 nm) co-existing with sinusoidal channel (0.53×0.56 nm) of HZ5(80). Straight channel HZ11(75) exhibited the less diffusion resistance than sinusoidal channel, which means that reactant and products can be easily passed through the channel of the HZ11(75). So, the reactions, such as aromatization, alkylation, H-transfer, and cracking, beyond the dehydration step could be prevented by a low contact time.

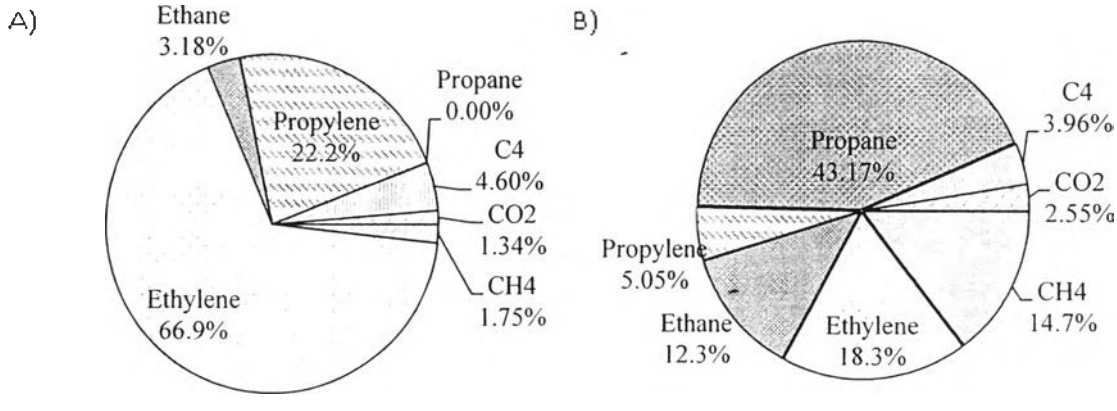

Figure 5.5 Composition of gas from using (A) HZ11(75), and (B) HZ5(80) as a catalyst.

The oil products from ethanol dehydration reaction are categorized into the petroleum fractions as shown in Figure 5.6. The main fraction is gasoline, which 71.7% and 87.7% is produced in oil by using HZ11(75) and HZ5(80), respectively, as the catalysts. The distillate-range products, kerosene and gasoil, are produced 28.2 wt. % in oil by using HZ11(75); however, HZ5(80) yields larger amount of gasoline-range product than HZ11(75) by 16.0%. LVGO and HVGO are

absent by both catalysts. The compositions of extracted oil by using HZ11(75) and HZ5(80) as the catalysts are shown in Figure 5.7. Xylenes, C9 aromatics, and C10+ aromatics products were the main components in the extracted oil. HZ5(80) prefers to produce C9 aromatics and C10+ aromatics; on the other hand, HZ11(75) prefers to produce xylenes. It is observed that the aromatics selectivity considered in terms of the BTEX/Aromatics and BTEX/Oil ratios by using HZ11(75) is higher than that of HZ5(80) as shown in Figure 5.8. The low diffusion resistance also affects the amount of BTEX products by obstructing further secondary reactions to large hydrocarbon products.

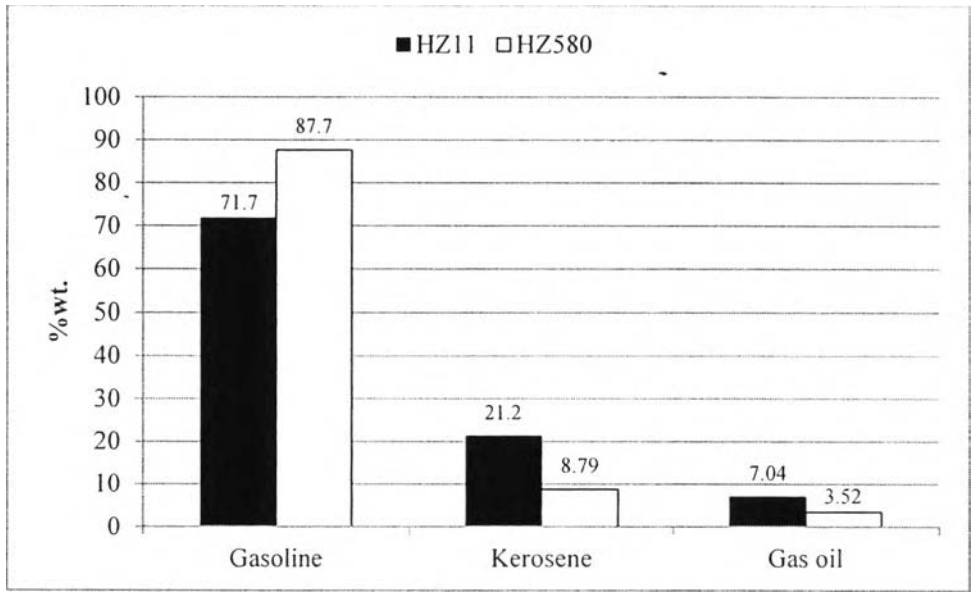

Figure 5.6 Petroleum fractions in extracted oils by using HZ5(80), and HZ11(75) catalysts.

Moreover, straight channel HZ11(75) also enhances *p*-xylene selectivity (*p*-xylene/xylenes = 0.27), compared with sinusoidal channel (*p*-xylene/xylenes = 0.16). Chen *et al.* (2013) revealed that the thermodynamic equilibrium of C8 aromatic isomers in xylene production from naphtha were 60 wt.% *m*-xylene, 14 wt.% *p*-xylene, 9 wt.% *o*-xylene, and 17 wt.% ethylbenzene, which the *p*-xylene/xylenes ratio is 0.17. HZ11(75) shows the *p*-xylene yield above the equilibrium condition.

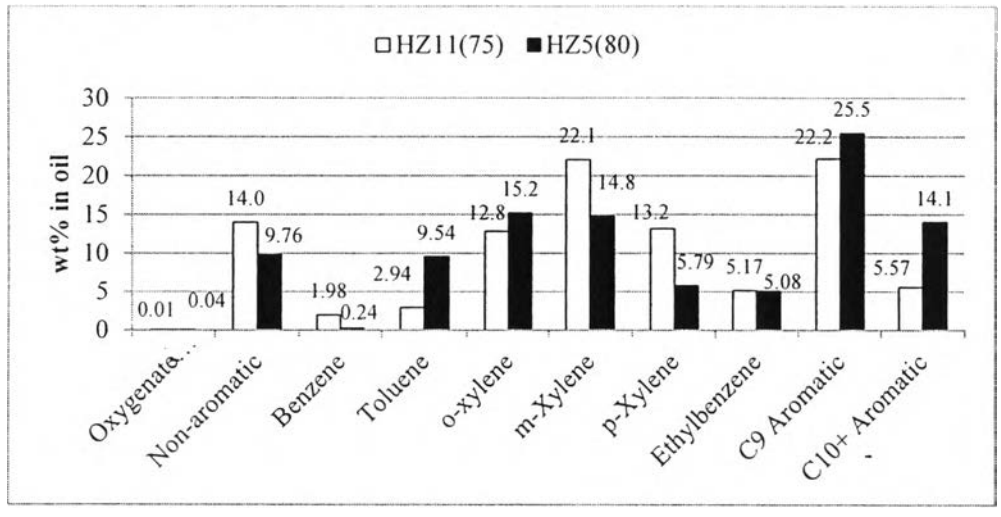

Figure 5.7 Composition of extracted oils by using HZ11(75), and HZ5(80) catalysts.

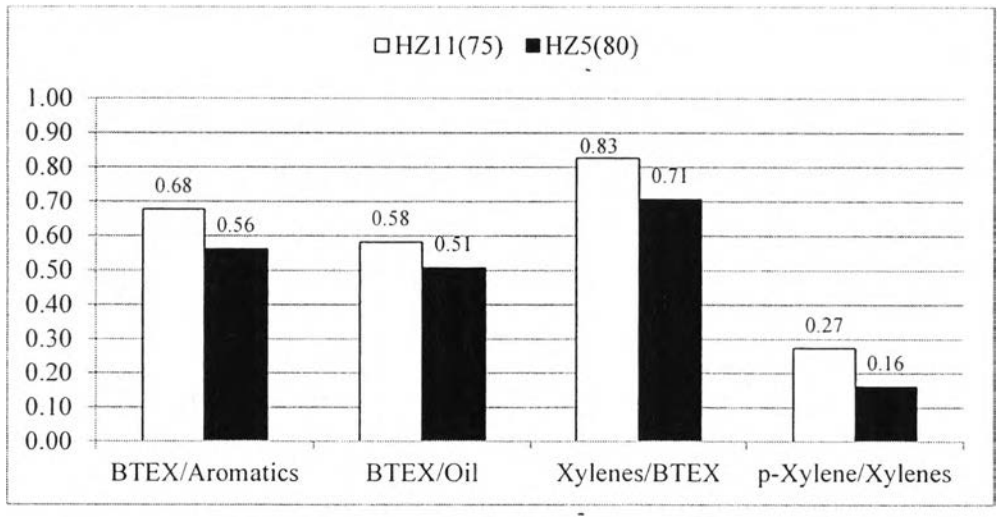

Figure 5.8 Ratio of BTEX/Aromatics, BTEX/Oil, xylenes/BTEX, and *p*-xylene/ xylenes by using HZ11(75), and HZ5(80) catalysts.

5.4.3 Effect of Phosphorus Oxide Promoter

Phosphorus oxide promoter is loaded to HZ11(75) and HZ5(80) catalysts. As shown in Figure 5.9, the oil yields are 4.30 wt.% and 4.41 wt.% by using HZ11(75) and HZ5(80) catalyst, respectively. The oil yield is decreased when phosphorus oxide is introduced to HZSM-5, but it is unchanged with using P/HZ11(75) as the catalyst. HZSM-11 has lower acid strength than HZSM-5, and the

phosphorus oxide that replaces the Bronsted acid sites of HZSM-11, slightly decreases the acid strength of the HZSM-11 support. So, the oil yield obtained from HZ5(80) decreases more than from HZ11(75). The conversion is improved slightly under the presence of phosphorus oxide. This also affects to gas composition by increasing ethylene yield, when phosphorus oxide is loaded.

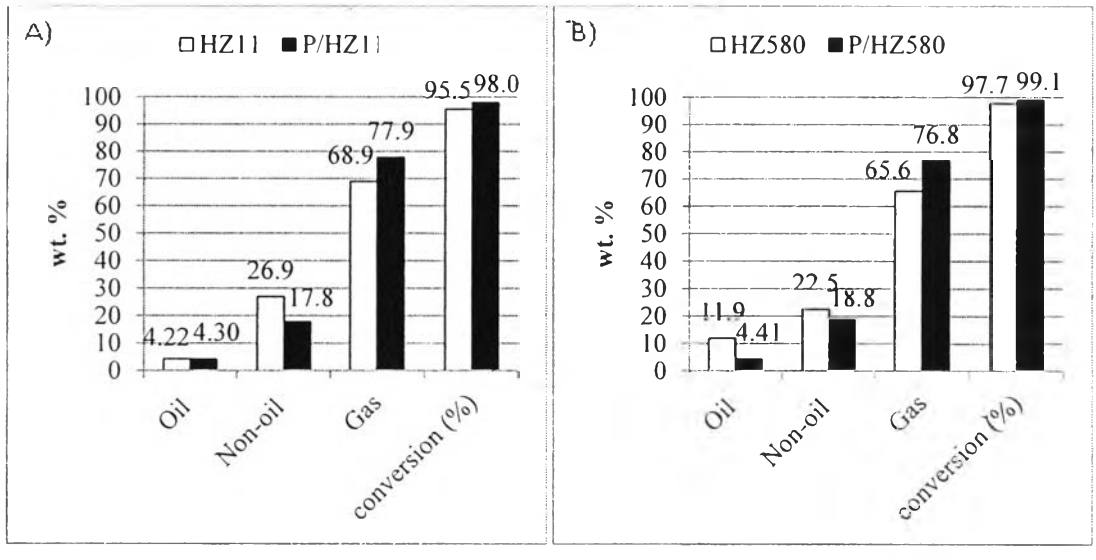

Figure 5.9 Product distribution and ethanol conversion from using (A) HZ11(75) and P/HZ11(75), and (B) P/HZ5(80) zeolite.

Ethylene is normally formed from the first step of dehydration process at a sufficiently high temperature (Inaba *et al.*, 2006). The strong acid sites are decreased because phosphorus oxide deposits on the sites. Takahashi *et al.* (2012) studied the P/Al atomic ratio in the range of 0-1 in phosphorus oxide-supported HZSM-5. They found that the phosphorus oxide promoter partially decreases strong acid site; moreover, at 1.0 P/Al ratio, the nearly absence of strong acid site is observed. At the 0.4 P/Al ratios, the results show the largest yield of propylene; moreover, ethylene yield was increased gradually with P/Al ratio, and ethylene yield was around 90% at 1.0 P/Al ratio. In this work, 73.7% and 98.6% yields of ethylene are produced by using P/HZ11(75) and that of P/HZ5(80) at a calculated P/Al of 3.27 and 3.48, respectively.

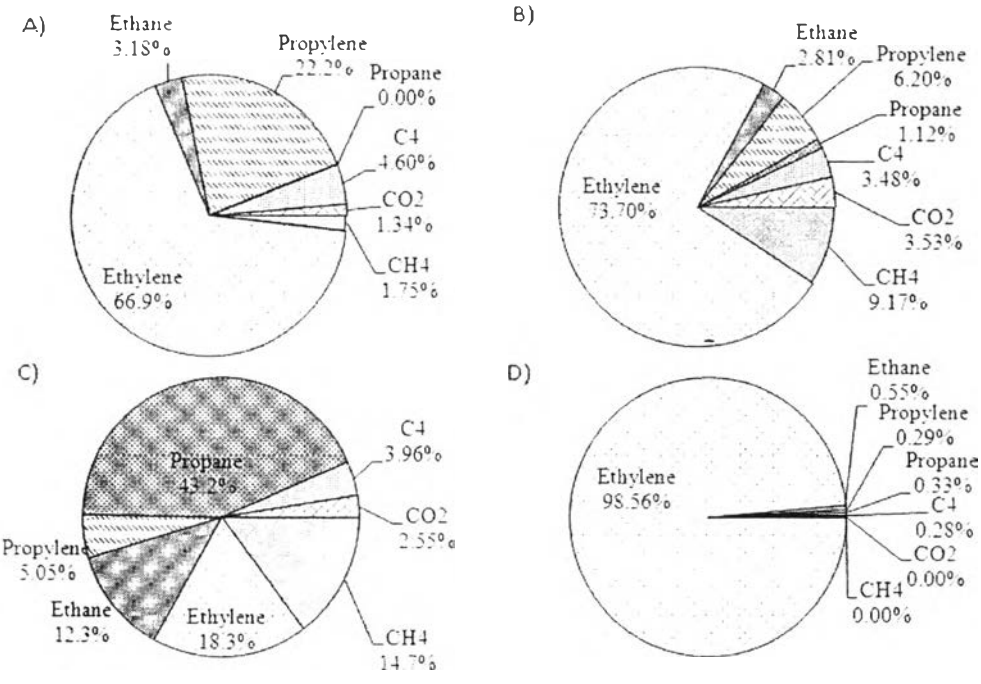

Figure 5.10 Composition of gas from using (A) HZ11(75), (B) P/HZ11(75), (C) HZ5(80), and (D) P/HZ5(80) catalysts.

Distillate range products (kerosene and gas oil) are improved by the presence of phosphorus oxide on HZSM-11 and HZSM-5 catalyst as shown in Figure 5.10; nevertheless, phosphorus oxide decreases the acid strength of zeolite, which results in the decreasing oil yield. On the other hand, phosphorus oxide can improve the oxygenate compounds in oil as shown in Figures 5.11 and 5.12.

As a result, 7.03 wt.% and 25.9 wt.% of oxygenate compounds in oil are obtained by using HZ11(75) and HZ5(80) as the catalyst, respectively. Moreover, C10+ aromatics, which are heavy hydrocarbons, are obtained at 7.49 wt.% and 44.4 wt.% by using HZ11(75) and HZ5(80), respectively, as the catalysts. The increasing C10+ aromatics and oxygenates in oil can drive the kerosene^{+}- range products (all ranges of hydrocarbon that are heavier than gasoline) to 40.8 wt.% and 73.6 wt.% by using HZ11(75) and HZ5(80), respectively. 44 wt.% C10+ aromatics obtained by using HZ5(75) contain C10-C12 indene and naphthalene derivatives, and some of benzene derivatives.

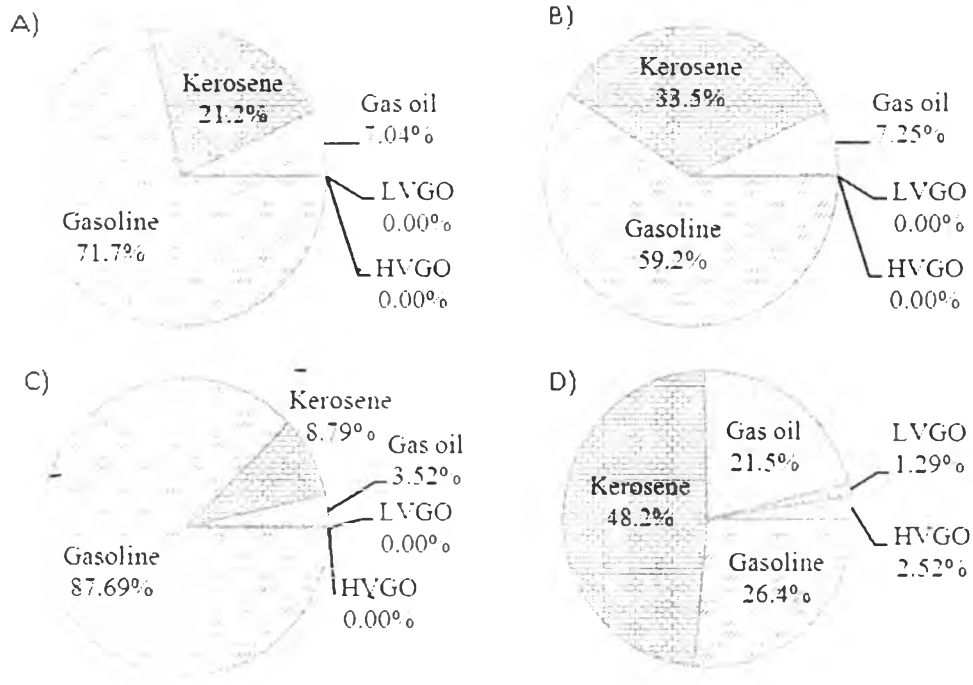

Figure 5.11 Petroleum fractions in extracted oils from using (A) HZ11(75), (B) P/HZ11(75), (C) HZ5(80), and (D) P/HZ5(80)catalysts.

With introducing phosphorus oxide to both zeolites, C10+ aromatics and oxygenates are improved, especially in P/HZ5(80) that gives 44 wt.% C10+ aromatics. *p*-xylene/xylenes is improved markedly to 0.4 on both modified zeolites due to the decreasing *o*-, and *m*- xylene and increasing p-xylene amounts. On the other hand, BTEX in oil and in aromatics are also decreased because the increasing C10+ aromatic and oxygenated compounds as can be seen in Figure 5.12 A, B, and C.

The production of oxygenates can be attributed to phosphorus oxide cluster located in the zeolite pore that decreases the Brönsted acid sites as illustrated in Figure 5.13. So, the weaker acid sites on the phosphorus oxide are proper to form the oxygenate products. Moreover, phosphorus oxide located outside the pore of zeolite is less than inside the pore because the capillary force drives the precursor solution of phosphorus oxide into the pores (confirmed by the reduction of Bronsted acid sites observed from TPD-IPA results).

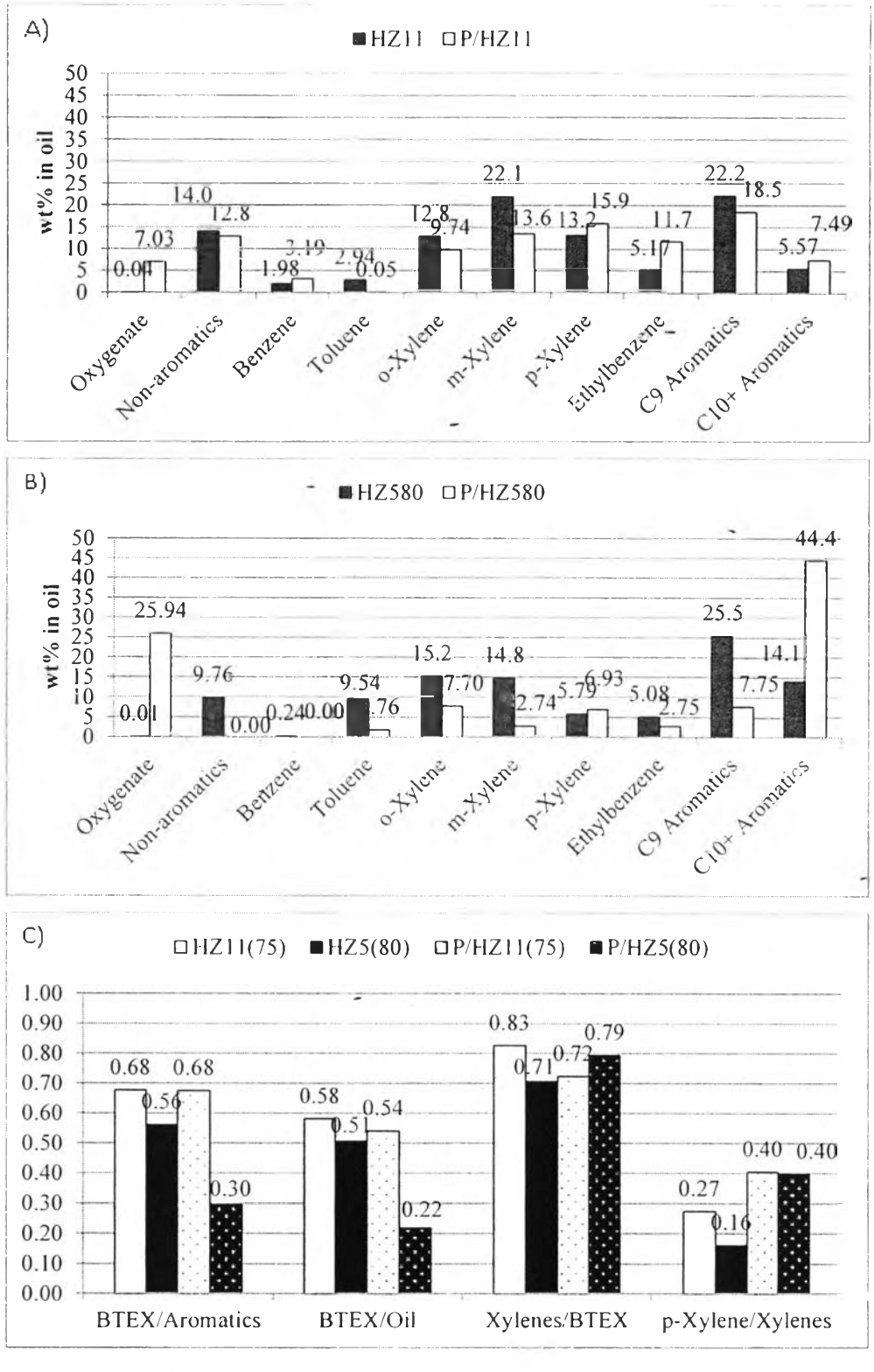

Figure 5.12 Composition of extracted oils from using (A) HZ11(75) and P/HZ11(75), (B)HZ5(80), and P/HZ5(80) catalysts.

In addition, diffusion constraint outside the pore is less than inside the pore; so, catalytic reactions can take place outside the pore, resulting in the increasing C10+ aromatics. Moreover, phosphorus oxide promoter can increase the acid strength that also enhances the C10+ aromatics formation.

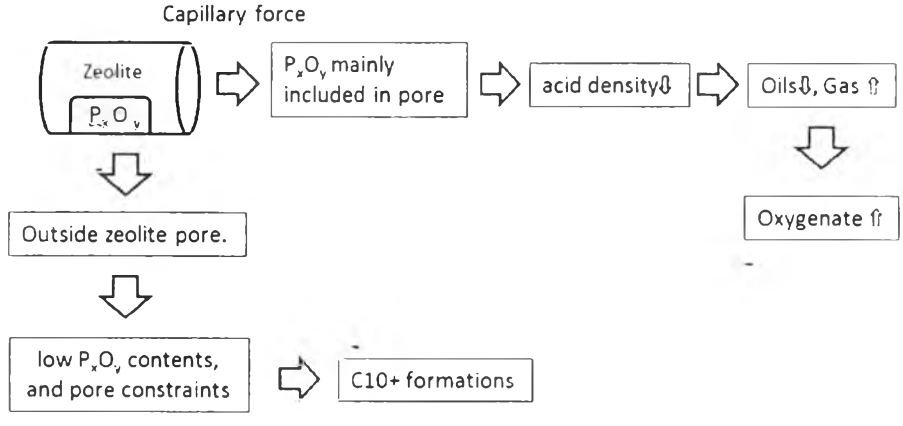

Figure 5.13 Effects of phosphorus oxide promoter on C10+ aromatics and oxygenate production.

5.4.4 Effect of Antimony Oxide Promoter

Bio-ethanol conversion seems to increase insignificantly, when antimony oxide is introduced to HZ11(75) and HZ5(80). Moreover, the gas yield is increased; in opposition, the yield of non-oil products are decreased as shown in Figure 5.14. The oil yield is increased from 11.9 wt.% to 13.8 wt.% by using Sb/HZ5(80), compared with pure HZ5(80), but the oil yield is slightly decreased from 4.22 wt.% to 3.75 wt.% by promoting HZ11(75) with antimony oxide promoter.

The gas compositions obtained by using zeolites with antimony oxide promoter seem to be the same as those obtained from the pure HZ11(75) and HZ5(80) zeolites. Ethylene and propylene are produced by using Sb/HZ11(75); on the other hand, propane is produced by using Sb/HZ5(80). Compared to unpromoted zeolite, ethylene selectivity is increased from 66.9 wt.% to 83.4 wt.% and 18.3 wt.% to 22.2 wt.% by using Sb/HZ11(75) and Sb/HZ5(80), respectively. Moreover, propylene selectivity is decreased from 22.3 wt.% to 13.5 wt.%; and similarly, propane is decreased from 43.2 wt.% to 35.5 wt.% by using Sb/HZ5(80) as the

catalyst. It can be noticed that antimony oxide bound to Brönsted acid sites of HZSM-5 partially affects to gas selectivity and oil yields (Li *et al.*, 2005).

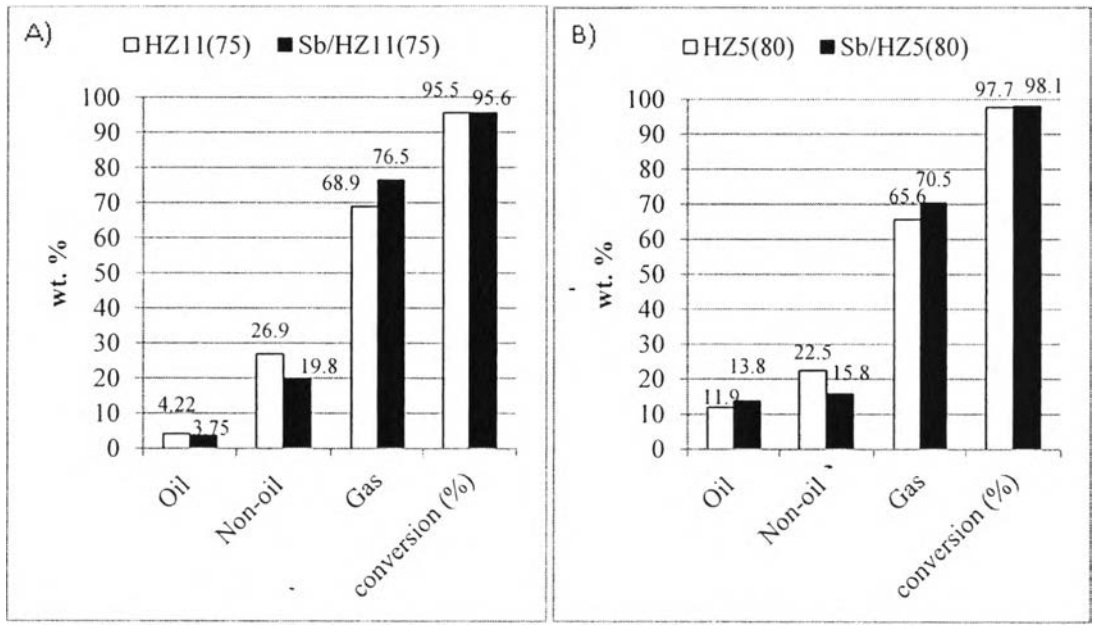

Figure 5.14 Product distribution and ethanol conversion from using (A) HZ11(75) and Sb/HZ11(75), and (B) HZ5(80) and Sb/HZ5(80) zeolite.

The trend of petroleum fractions in oils seems to be unchanged. Slightly increasing gasoline fraction is found in association with partial decrease in kerosene as shown in Figure 5.15. With the promotion of Sb, gasoline selectivity is increased from 71.7 wt.% to 75.6 wt. by using Sb/HZ11(75), and, 87.7 wt.% to 90.0 wt.% by using Sb/HZ5(80).

In addition, the compositions of extracted oil are shown in Figure 5.16. Sb/HZ11(75) and Sb/HZ5(80) give nearly the same oil composition. Compared to pure HZ11(75) and HZ5(80), benzene and toluene are increased; but C9 and C10+ aromatics are decreased by using Sb/HZ11(75) and Sb/HZ5(80).

Using Sb/HZ5(80), o-xylene and m-xylene selectivity are dropped, but only *p*-xylene is increased. Moreover, benzene, toluene, and ethylbenzene are increased evidently. This can be explained by the effect of pore narrowing with introducing the antimony oxide to the zeolite, resulting in the enhancement of para-

selectivity and mono-substituted molecules (Zheng *et al.*, 2003). The explanation can be depicted to the diagram as shown in Figure 5.17.

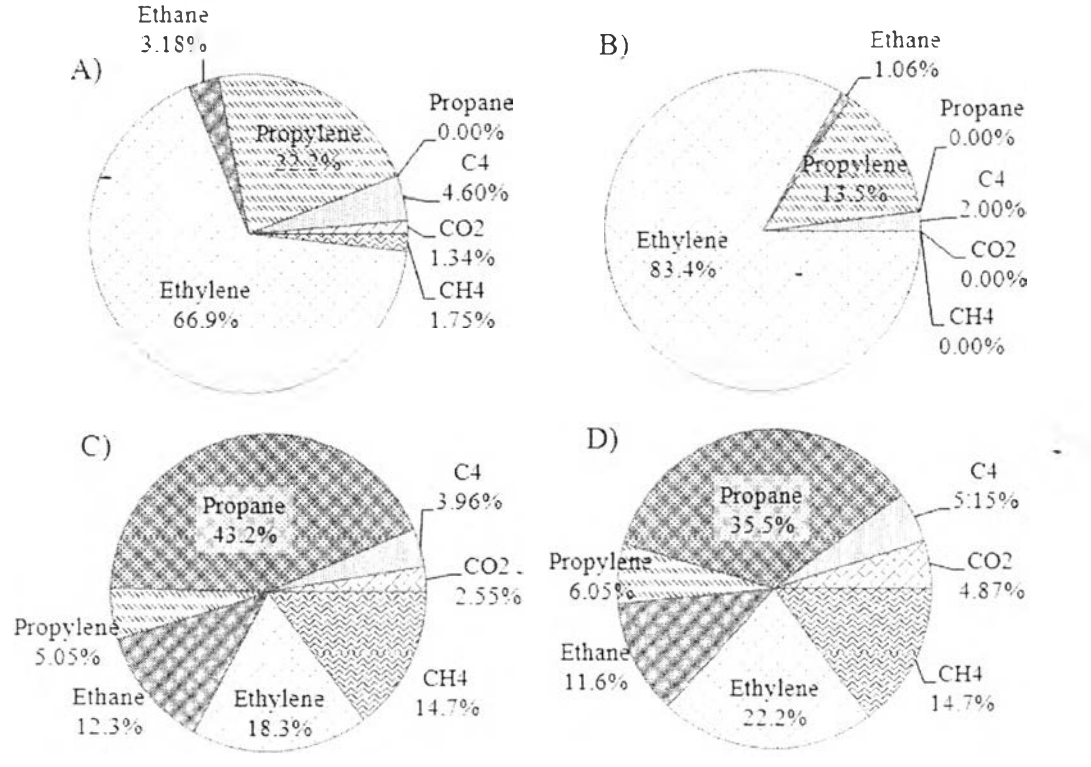

Figure 5.15 Compositions of gas from using (A) HZ11(75), (B) Sb/HZ11(75), (C) HZ5(80), and (D) Sb/HZ5(80) catalysts.

C9 and C10+ aromatics are decreased with promotion with antimony oxide promoter. Moreover, Sb/HZ5(80) gives 10.2 wt.% *o*-xylene and 12.3 wt.% *p*-xylene; but, Sb/HZ11(75) gives the same composition of xylene isomers, compared to that of pure HZ11(75) as shown in Figure 5.18. This can be noticed that the diffusion constraint of sinusoidal channel structure with antimony oxide promoter could faintly produce of ortho- and meta- selectivity. So, the *p*-xylene/xylenes ratio are improved evidently to 0.46 by using Sb/HZ5(80) as can be seen in Figure 5.18C. It is interesting that Sb/HZ11(75) can improve the BTEX/oils ratio to 0.92 because it can suppress C9, C10+ aromatics and non-aromatics formation.

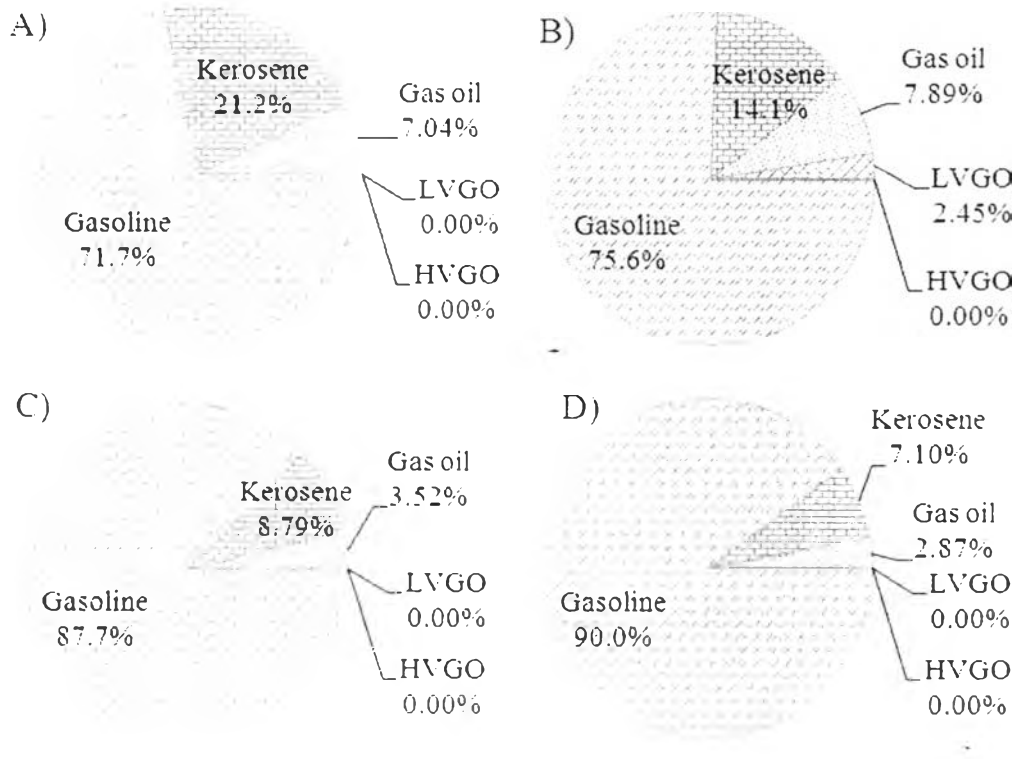

Figure 5.16 Petroleum fractions in extracted oils by using (A) HZ11(75), (B) Sb/HZ11(75), (C) HZ5(80), and (D) Sb/HZ5(80) catalysts.

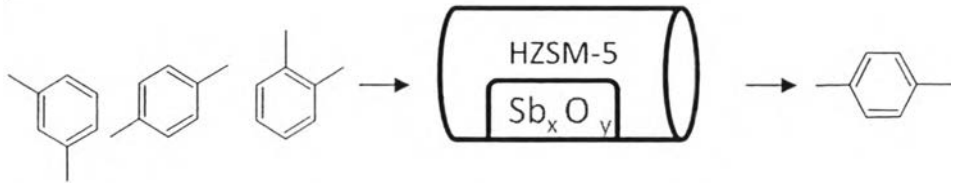

Figure 5.17 Product shape selectivity of Sb/zeolites.

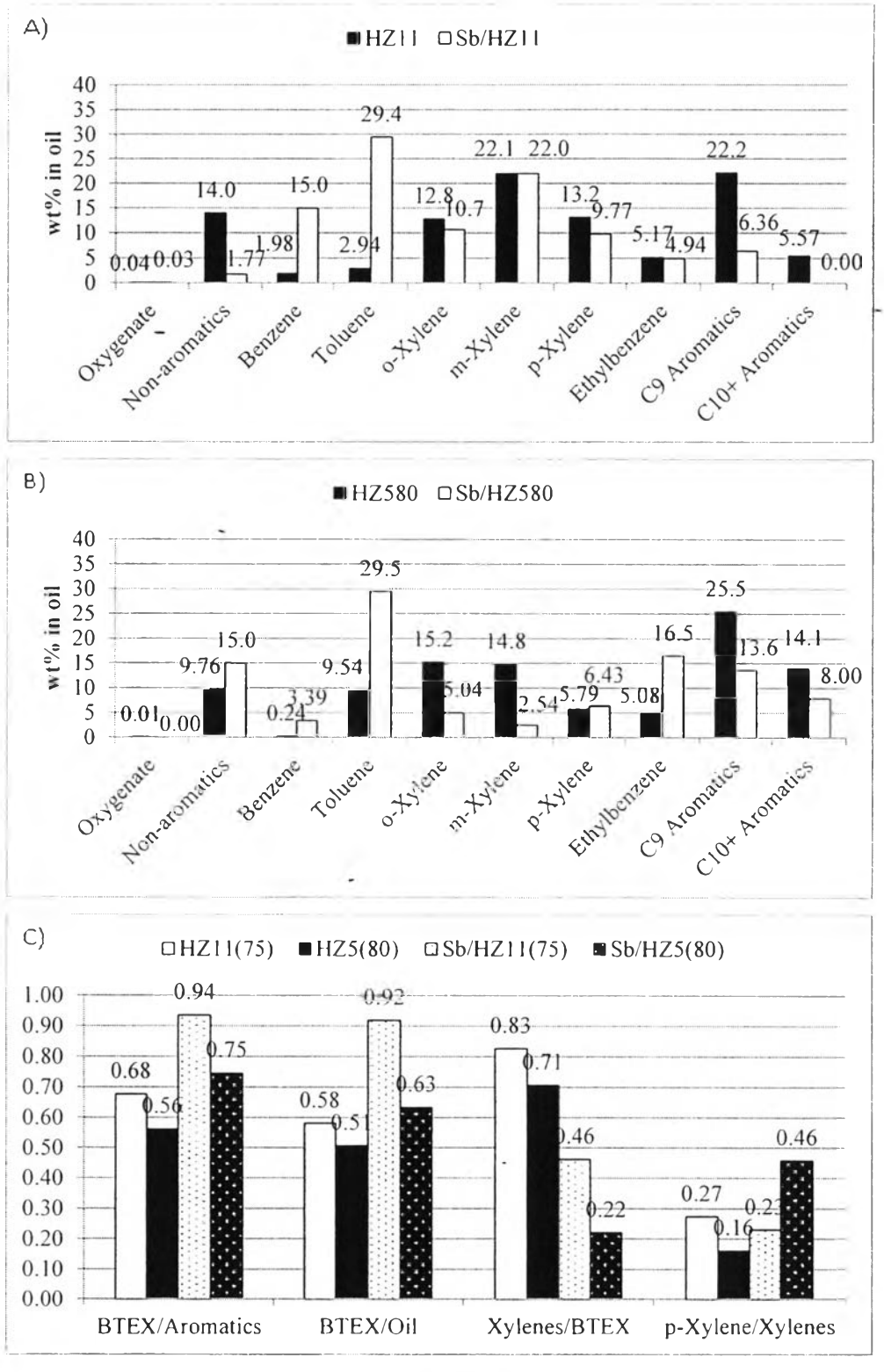

Figure 5.18 Composition of extracted oils from using (A) HZ11(75) and Sb/HZ11(75), (B) HZ5(80), and Sb/HZ5(80) catalysts, and (C) ratio of BTEX products.

5.4.5 Effect of Bismuth Oxide Promoter

Compared with the pure zeolites, the oil yields are increased for 0.17 wt.% and 6.43 wt.% by using Bi/HZ11(75) and Bi/HZ5(80), respectively. The bio-ethanol conversion also increases at the presence of bismuth oxide as shown in Figure 5.19 A and B.

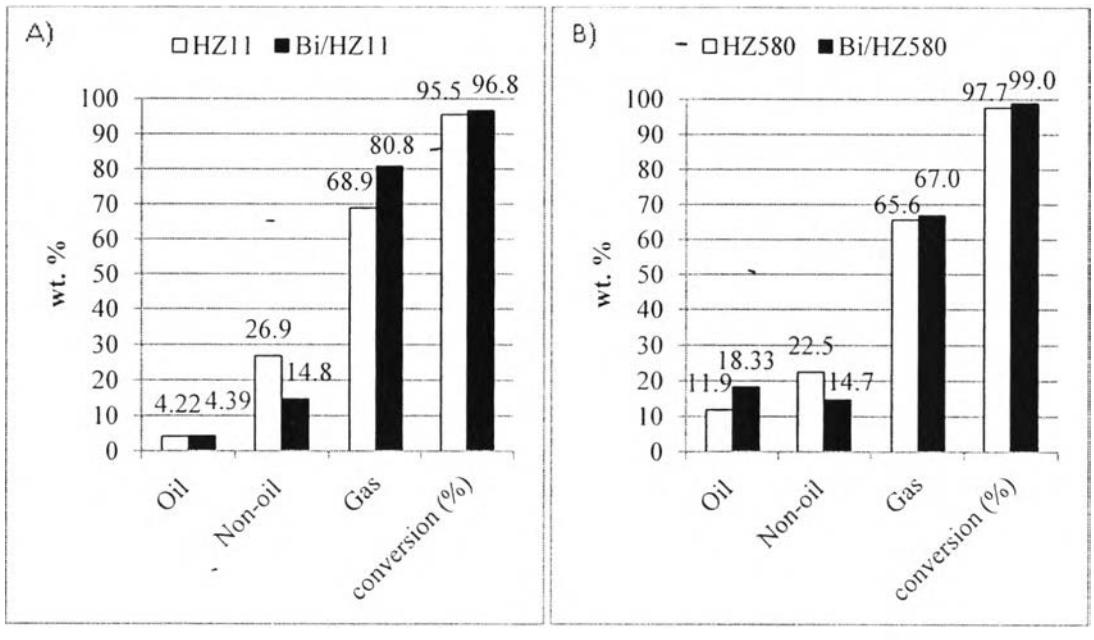

Figure 5.19 Product distribution and ethanol conversion from using (A) HZ11(75) and Bi/HZ11(75), and (B) HZ5(80) and Bi/HZ5(80).

The compositions of gas products obtained from using Bi/HZ11(75) and HZ5(80) are the same as those obtained from the pure zeolites as shown in Figure 5.20. Propylene selectivity is decreased; on the other hand, ethylene yields is increased by using Bi/HZ11(75), compared with HZ11(75). Moreover, ethylene and ethane are increased; conversely, propane is decreased by using Bi/HZ5(80), compared with HZ5(80). Propane is still absent using both HZ11(75) and Bi/HZ11(75). Moreover, the gas product obtained by using Sb/HZ11(75) is free of low value gas such as CO_2, methane, and propane, which is an advantage for commercial process.

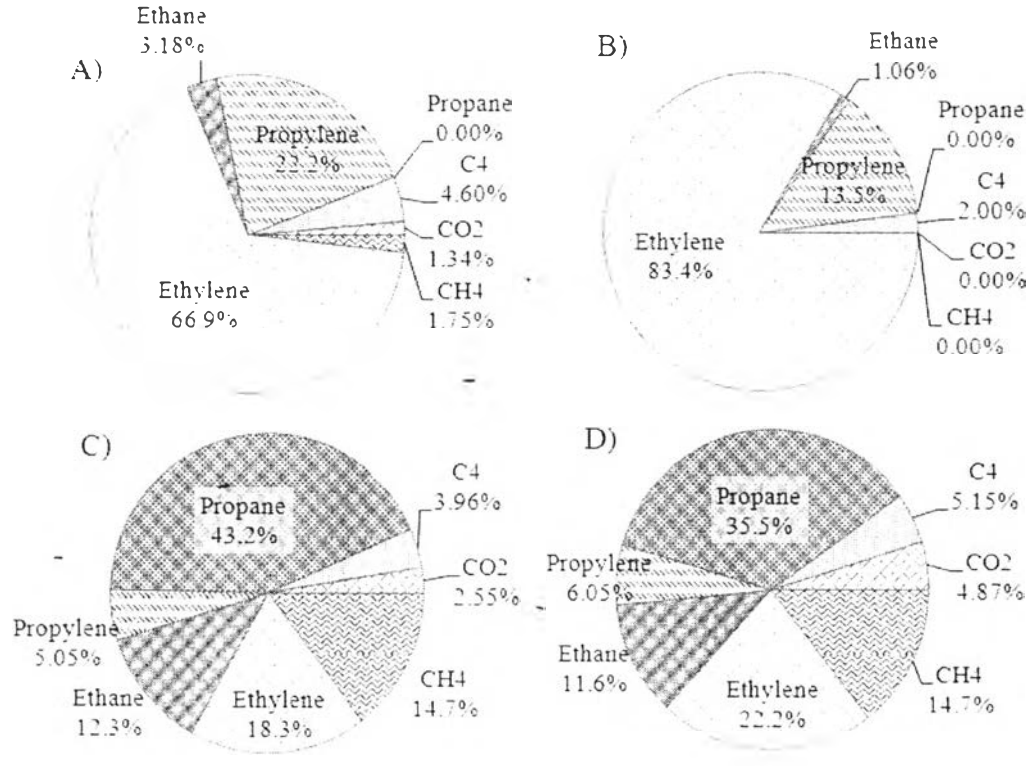

Figure 5.20 Composition of gas products from using (A) HZ11(75), (B) Sb/HZ11(75), (C) HZ5(80), and D) Sb/HZ5(80) catalysts.

The petroleum fractions in oil are shown in Figure 5.21. Kerosene and gas oil are decreased; on the other hand, gasoline is increased for 9.71% in case of Bi/HZ11(75), compared with Bi/HZ11(75). However, kerosene yield is increased while gasoline is decreased by using Bi/HZ5(80), compared with HZ5(80). LVGO and HVGO are still absent even with using Bi-oxide modified catalyst.

BTEX products are increased; on the other hand, C9, C10+ aromatics, and non-aromatics are decreased by using Bi/HZ11(75), compared with HZ11(75). This is a strong point for commercial process. It can be explained that bismuth oxide can help to generate more aromatic products by enhancing dehydrocyclization and aromatization on its Lewis acid site (Dumitriu *et al.*, 2003). So, the oil yield and BTEX products are improved. Non-aromatics seem to be converted to aromatics products. C9 and C10+ aromatics, which tend to occur outside the pore of zeolite, are decreased, which could be explained by the partial substitution of external acid sites by the metal oxide with higher acid strength.

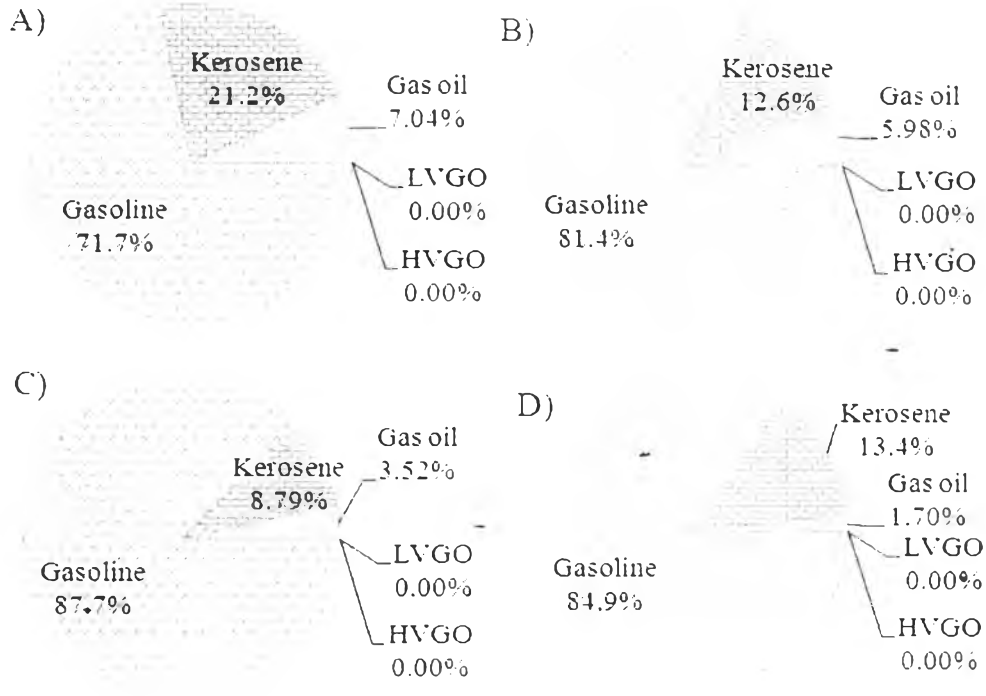

Figure 5.21 Petroleum fractions in extracted oils by using (A)HZ11(75), (B)Bi/HZ11(75), (C)HZ5(80), and (D)Bi/HZ5(80) catalysts.

With loading Bi oxides to HZ5(80), non-aromatics are increased significantly. This can be explained that dehydrocyclization and aromatization are occurred dominantly. So, the non-aromatics, which are 1,5-heptadiene-3-yne, are produced in the large extents with no cycloalkane and cycloalkene formation. This can be explained that the high acid strength of bismuth oxide can convert cycloalkanes and cycloalkenes to aromatics via dehydrocyclization and aromatization. Moreover, high acid strength also promotes cracking reaction, resulting in a large amount of 1,5-heptadiene-3-yne production (20.73% in oil). Ethylbenzene could be produced on ZSM-5 by the reaction between benzene and ethanol at a high temperature. Yuan and Gevert (2004) revealed that 28.05% ethylbenzene was produced by using HZSM-5(SiO_2/Al_2O_3 = 62) at 500 °C with benzene:ethanol ratio equal to 2:1.

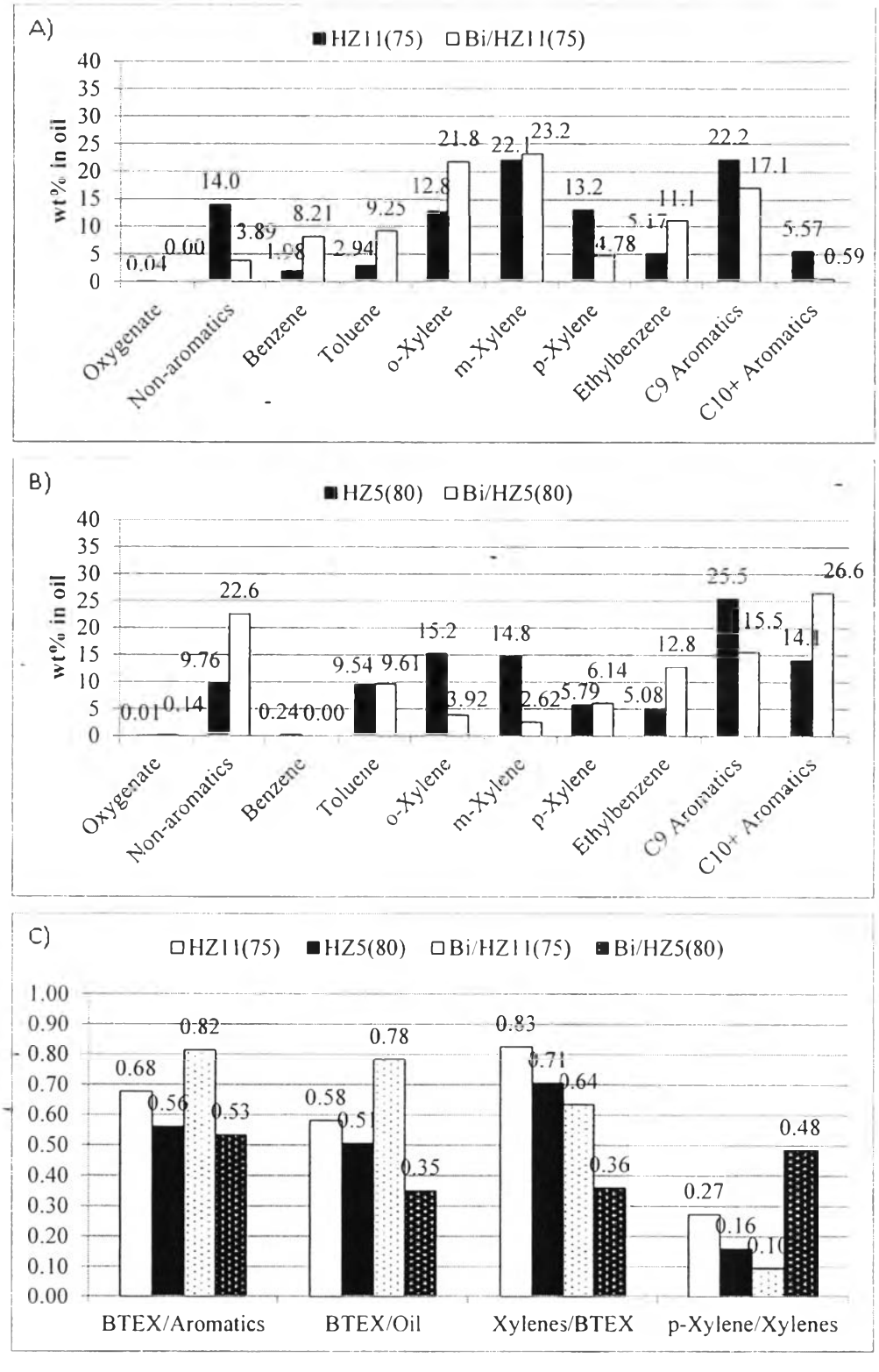

Figure 5.22 Composition of extracted oils from using (A)HZ11(75) and Sb/HZ11(75), (B)HZ5(80), and Sb/HZ5(80) catalysts, and (C) ratio of BTEX products.

P-xylene/xylenes ratio is enhanced by using Bi/HZ5(80) to 0.48. On the other hand, Bi/HZ11(75) tends to increase the production of overall BTEX product, which are the same as using antimony-oxide modified catalysts.

5.4.6 Effect of Oxide Species on Product Distributions

The product distribution is affected by introducing P-, Sb-, and Bi-oxides to the zeolite supports. Generally, product distribution is governed by acid properties, SiO_2/Al_2O_3, pore size and pore channel structure. In this case, these acidic oxides bound to the Brönsted acid sites of zeolite can exhibit the new Brönsted acid sites with the decrease in conventional Brönsted acid sites. Their acid strength depends on the acid properties of these oxides. The larger the atomic number of group 5A oxide, the more acid strength is exhibited. Phosphorus oxide promoter is the smallest in size among those of group 5A. The quantity of a small size oxide are higher than a large size oxide at the same weight of loading and cause the decrease of Brönsted acid site that is necessary for protonation hydrocarbons to form the larger hydrocarbons. On the other hand, C10+ aromatics are produced in a large extent because they can be formed outside the pore that have lower amounts of phosphorus oxide. The oil yield is decreased with using phosphorus oxide as a promoter. Moreover, the acid sites of P/HZ11(75) and P/HZ5(80) are proper to produce oxygenate compounds. Antimony oxide and bismuth oxide promoters can help in dehydrocyclization and aromatization, as confirmed by high aromatic oil yield. The reaction pathway of dehydrocyclization and aromatization are exhibited in Figure 5.23.

Moreover, Diels Alders mechanism is also used to explain the cyclization and aromatization reactions, which are shown in Figure 5.24. The formation of butadiene can be taken place by the reaction between acetaldehyde and ethanol as shown in Figure 5.25, or it can be produced by hydrogen transfer to butene.

So, the oil yield is improved by using antimony oxide- and bismuth oxide-modified catalysts. Moreover, these oxides can act like pore narrowing agents, and increase the para- and mono-substituted aromatic hydrocarbons. In addition, cracking reaction also occurs in case of using bismuth oxide promoter.

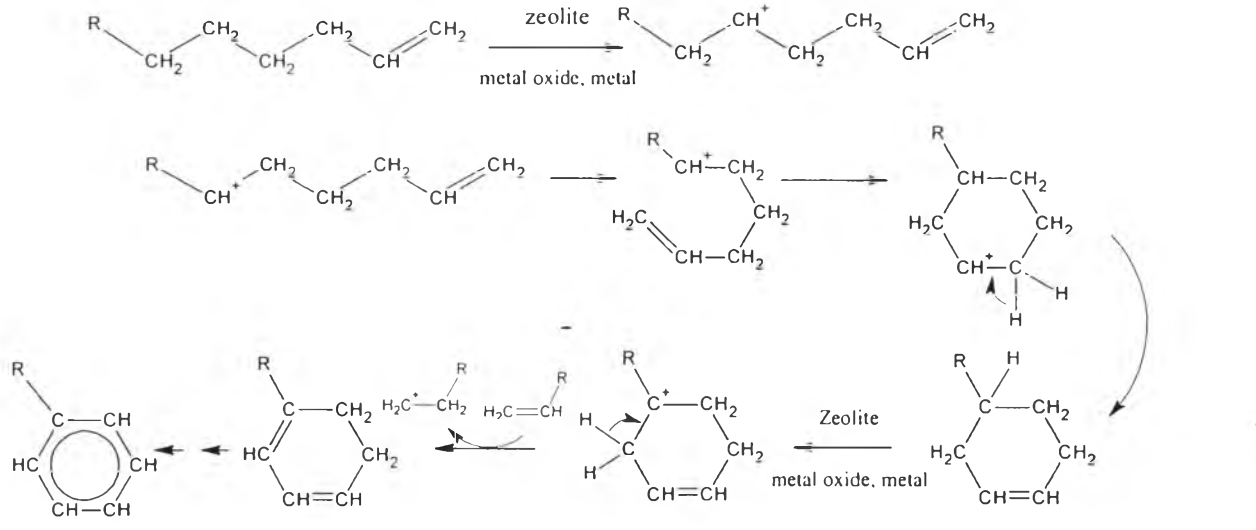

Figure 5.23 Hydride abstraction, dehydrocyclization, and aromatization of an alkene (Resasco, 2000).

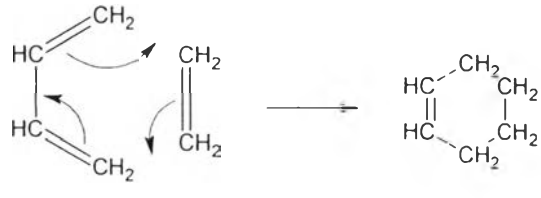

Figure 5.24 An Diels Alders reaction (Cole *et al.*, 1984; Ian Hunt, 2006).

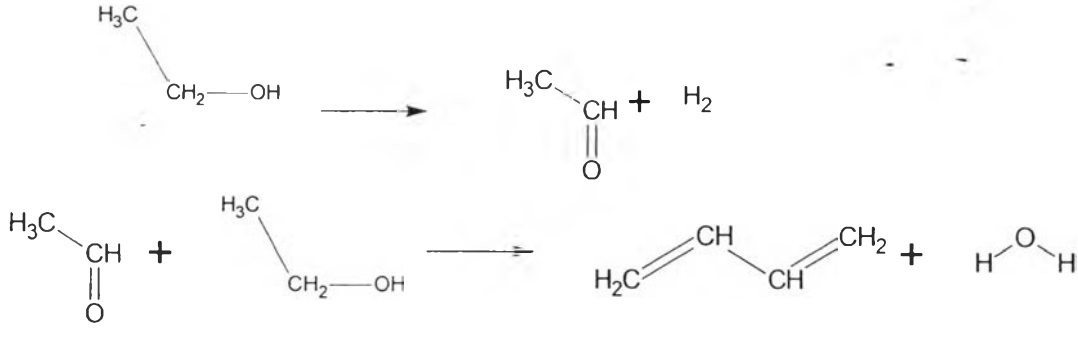

Figure 5.25 Conversion of ethanol to butadiene (Jones *et al.*, 1949).

5.5 Conclusions

The oil yield were found to be governed by the complexity of the pore and acid strength. Moreover, P-, Sb-, and Bi- oxides can improve the oil yield because their high Brönsted acid sites helped in dehydrocyclization and aromatization. The oil yield was decreased with using P/HZ5(80) and P/HZ11(75); on the other hand, oxygenates and C10+ aromatics were more produced. Mono-, and para- substituted molecules with increased when using Sb/HZ5(80) and Sb/HZ11(75). Moreover, BTEX was improved with using Bi/HZ11(75), but Bi/HZ5(80) tended to produce non-aromatics.

5.6 Acknowledgements

The authors would like to thank the Center of Excellence on Petrochemical and Materials Technology, TOP-PPC R&D Collaboration Unit, and The Petroleum and Petrochemicals College, Chulalongkorn University for the mutual financial support and Sapthip Company Limited for bio-ethanol used in this work.

5.7 References

Baerlocher, C., and McCusker, L.B. "Zeolite structure." Izasc-mirror. 17 Nov 2013 <http://izasc-mirror.la.asu.edu/fmi/xsl/IZA-SC/ft.xsl>

Beck, J.S., and Schlenker, J.D. (1993) U.S. Patent 5 213 786

Chen, C.Y., Liang, A.J.B., Miller, S.J., and Ziemer, J.N. (2013) U.S. Patent 8 471 083

Chu, P., Woodbury, and N.J (1973) U.S. Patent 3 709 979

Cole, J.A., Bittner, J.D., Longwell, J.P., and Howard, J.B. (1984) Formation mechanisms of aromatic compounds in aliphatic flames. Combustion and Flame, 56(1), 51-70.

Dumitriu, D., Bârjega, R., L. Frunza, D. Macovei, T. Hu, Y. Xie, V.I. Pârvulescu, and Kaliaguine, S. (2003) BiOx clusters occluded in a ZSM-5 matrix: preparation, characterization, and catalytic behavior in liquid-phase oxidation of hydrocarbons. Journal of Catalysis, 219, 337-351.

Feng-Yuen, D., Minoru, S., Hiroshi, T., and Yasukazu, S. (1988) XRD characteristic of Na-ZSM-5 synthesized from an organic-free system. Bulletin of the Chemical Society of Japan, 61, 3404.

Goto, D., Harada, Y., Furumoto, Y., Takahashi, A., Fujitani, T., Oumi, Y., Sadakane, M., and Sano, T. (2010) Conversion of ethanol to propylene over HZSM-5 type zeolites containing alkaline earth metals. Applied Catalysis A: General, 383(1–2), 89-95.

Gu, Y., Cui, N., Yu, Q., Li, C., and Cui, Q. (2012) Study on the influence of channel structure properties in the dehydration of glycerol to acrolein over H-zeolite catalysts. Applied Catalysis A: General, 429-430(0), 9-16.

Ian Hunt "Diels-Alder Reaction." 13 Mar 2014 <http://www.chem.ucalgary.ca/courses/ 351/Carey5th/Ch10/ch10-5.html>

Inaba, M., Murata, K., Saito, M., and Takahara, I. (2006) Ethanol conversion to aromatic hydrocarbons over several zeolite catalysts Reaction Kinetics and Catalysis Letters, 88(1), 135-141.

Jones, H.E., Stahly, E.E., and Corson, B.B. (1949) Butadiene from Ethanol. Reaction Mechanism. Journal of the American Chemical Society, 71(5), 1822-1828.

Li, B., Li, S., Wang, Y., Li, N., Liu, X., and Lin, B. (2005) Study on antimony oxide self-assembled inside HZSM-5. Journal of Solid State Chemistry, 178(4), 1030-1037.

Li, Y., Cheng, J., Song, J., Alonso, J.A., Fernández-Díaz, M.T., and Goodenough, J.B. (2012) Characterization of the Double Perovskite Ba2BixSc0.2Co1.8–xO6−δ (x = 0.1, 0.2). Chemistry of Materials, 24(21), 4114-4122.

Lu, J., Liu, Y., and Li, N. (2011) Fe-modified HZSM-5 catalysts for ethanol conversion into light olefins. Journal of Natural Gas Chemistry, 20(4), 423-427.

Moulder, J.F., Stickle, W.F., Sobol, P.E., and Bomben, k.B. (1992) Handbook of X-ray photoelectron spectroscopy: Perkin-Elmer corporation.

Pasomsub, S. (2013) Bio-ethanol dehydration to liquid hydrocarbons. M.S. Thesis, The petroleum and Petrochemical College, Chulalongkorn, Chulalongkorn University, Bangkok, Thailand.

Resasco, D.E. (2000) Dehydrogenation by Heterogeneous Catalysts. School of Chemical Engineering and Materials Science, University of Oklahoma.

Takahashi, A., Xia, W., Nakamura, I., Shimada, H., and Fujitani, T. (2012) Effects of added phosphorus on conversion of ethanol to propylene over ZSM-5 catalysts. Applied Catalysis A: General, 423-424(0), 162-167.

Varvarin, A.M., Khomenko, K.M., and Brei, V.V. (2013) Conversion of n-butanol to hydrocarbons over H-ZSM-5, H-ZSM-11, H-L and H-Y zeolites. Fuel, 106(0), 617-620.

Viswanadham, N., Saxena, S.K., Kumar, J., Sreenivasulu, P., and Nandan, D. (2012) Catalytic performance of nano crystalline H-ZSM-5 in ethanol to gasoline (ETG) reaction. Fuel, 95(0), 298-304.

Wongwanichsin, P. (2013) Modified SAPO-34 for dehydration of Bio-ethanol to Light Olefins in Comparison with KOH-Treated HZSM-5. M.S. Thesis, The petroleum and Petrochemical College, Chulalongkorn, Chulalongkorn university, Bangkok, Thailand.

Yuan, J.-J., and Gevert, B.S. (2004) Alkylation of benzene with ethanol over ZSM-5 catalyst with different SiO_2/Al_2O_3 ratios. Indian Journal of Chemical Technology, 11, 337-345.

Zhang, L., Liu, H., Li, X., Xie, S., Wang, Y., Xin, W., Liu, S., and Xu, L. (2010) Differences between ZSM-5 and ZSM-11 zeolite catalysts in 1-hexene aromatization and isomerization. Fuel Processing Technology, 91(5), 449-455.

Zhang, L., Wu, J., Chen, F., Li, X., Schoenung, J.M., and Shen, Q. (2013) Spark plasma sintering of antimony-doped tin oxide (ATO) nanoceramics with high density and enhanced electrical conductivity. Journal of Asian Ceramic Societies, 1(1), 114-119.

Zheng, S., Jentys, A., and Lercher, J.A. (2003) On the enhanced para-selectivity of HZSM-5 modified by antimony oxide. Journal of Catalysis, 219(2), 310-319.